The Journal of Immunology

Galectin-3: A Positive Regulator of Leukocyte Recruitment in the Inflamed Microcirculation

Beatrice R. Gittens, Jennifer V. Bodkin, Sussan Nourshargh, Mauro Perretti and Dianne Cooper

J Immunol 2017; 198:4458-4469; Prepublished online 24 April 2017;
doi: 10.4049/jimmunol.1600709
http://www.jimmunol.org/content/198/11/4458

The Journal of Immunology is published twice each month by
The American Association of Immunologists, Inc.,
1451 Rockville Pike, Suite 650, Rockville, MD 20852

Print ISSN: 0022-1767 Online ISSN: 1550-6606.

Galectin-3: A Positive Regulator of Leukocyte Recruitment in the Inflamed Microcirculation

Beatrice R. Gittens, Jennifer V. Bodkin, Sussan Nourshargh, Mauro Perretti, and Dianne Cooper

In vivo and ex vivo imaging were used to investigate the function of galectin-3 (Gal-3) during the process of leukocyte recruitment to the inflamed microcirculation. The cremasteric microcirculation of wild-type (C57BL/6), Gal-3$^{-/-}$, and CX$_3$CR1$^{gfp/+}$ mice were assessed by intravital microscopy after PBS, IL-1β, TNF-α, or recombinant Gal-3 treatment. These cellular responses were investigated further using flow-chamber assays, confocal microscopy, flow cytometry, PCR analysis, and proteome array. We show that mechanisms mediating leukocyte slow rolling and emigration are impaired in Gal-3$^{-/-}$ mice, which could be because of impaired expression of cell adhesion molecules and an altered cell surface glycoproteome. Local (intrascrotal) administration of recombinant Gal-3 to wild-type mice resulted in a dose-dependent reduction in rolling velocity associated with increased numbers of adherent and emigrated leukocytes, ∼50% of which were Ly6G$^+$ neutrophils. Intrascrotal administration of Gal-3 to CX$_3$CR1$^{gfp/+}$ mice confirmed that approximately equal numbers of monocytes are also recruited in response to this lectin. Exogenous Gal-3 treatment was accompanied by increased proinflammatory cytokines and chemokines within the local tissue. In conclusion, this study unveils novel biology for both exogenous and endogenous Gal-3 in promoting leukocyte recruitment during acute inflammation. ***The Journal of Immunology*****, 2017, 198: 4458–4469.**

Inflammation is a vital response to tissue injury or infection. Its effectiveness relies on the trafficking of leukocytes, predominantly neutrophils initially, to the site of injury. In acute inflammation this neutrophilic infiltrate is short-lived due to the coordinated release of proresolution mediators that terminate neutrophil recruitment and promote their efferocytosis, leading to a return to homeostasis (1, 2). In chronic inflammation this resolution process fails and the leukocytic infiltrate becomes persistent, with, in the case of pathologies such as rheumatoid arthritis, repeated infiltration of neutrophils into the inflamed joint (3). Understanding the mechanisms by which leukocytes traffic from the bloodstream to the inflammatory site has been the focus of intense research over the past two decades, and the leukocyte recruitment cascade is now a well-defined paradigm (4, 5). Although many of the adhesion molecules that drive this process have been identified, it is evident that leukocyte recruitment is multifactorial and relies on the coordinated actions of many lipids and proteins including cytokines and chemokines, as well as the adhesion molecules themselves. Galectins represent a family of proteins that have been ascribed proadhesive and chemotactic properties; however, their role in neutrophil trafficking has not been systematically studied. In this article, we have focused on galectin-3 (Gal-3), a molecule thought to have predominantly proinflammatory functions.

Galectins are a family of β-galactoside binding proteins that elicit their effects by binding to exposed *N*-acetyllactosamine residues on cells (6). Specifically, Gal-3 binds glycoproteins that have been posttranslationally modified by the glycosyltransferase Mgat5 (β1,6-*N*-acetylglucosaminyl transferase 5), which is responsible for the addition of β1,6 branched *N*-acetylglucosamine to the α-linked mannose of biantennary N-linked oligosaccharides (7). Since its characterization, Gal-3 has been implicated in a range of pathologies, many of which involve both acute and chronic inflammatory responses characterized by neutrophil infiltration. Levels of Gal-3 are increased during inflammation, both systemically and locally at the inflammatory site. In rheumatoid arthritis, Gal-3 localizes to sites of joint destruction in the synovium, with increased levels of the protein also found in sera and synovial fluids when compared with those from healthy control subjects or osteoarthritis patients (8). Circulating Gal-3 is also detectable in the sera of patients with Behcet's disease and heart failure with levels of this lectin in excess of 50 ng/ml detectable (9, 10). In murine models of inflammation, elevated levels of Gal-3 in exudates have been found to correlate with increased neutrophil recruitment to the inflammatory site (11).

Because of its increased production during inflammation and the correlation between the presence of Gal-3 in inflammatory exudates and neutrophil infiltration, we sought to determine whether Gal-3 directly modulates the leukocyte recruitment process undertaken by neutrophils as they traffic from the blood to the tissue. We have addressed the role of both the endogenous protein, through the use of Gal-3 null mice, as well as the function of the recombinant protein. We have demonstrated for the first time, to our knowledge, that endogenous Gal-3 is specifically involved in leukocyte slow rolling and that the recombinant protein initiates recruitment of both neutrophils and monocytes to the cremaster microcirculation in an in vivo model of inflammation.

William Harvey Research Institute, Barts and The London School of Medicine and Dentistry, Queen Mary University of London, London EC1M 6BQ, United Kingdom

ORCIDs: 0000-0003-2068-3331 (M.P.); 0000-0002-5553-9447 (D.C.).

Received for publication May 10, 2016. Accepted for publication March 23, 2017.

This work was supported by funds from Arthritis Research UK (Fellowship 18103 to D.C.). B.R.G. was supported by a British Heart Foundation Ph.D. studentship (Grant FS/10/009/28166). S.N. and J.V.B. were funded by the Wellcome Trust (Grant 098291/Z/12/Z to S.N.).

Address correspondence and reprint requests to Dr. Dianne Cooper, William Harvey Research Institute, Barts and The London School of Medicine and Dentistry, Queen Mary University of London, Charterhouse Square, London EC1M 6BQ, U.K. E-mail address: d.cooper@qmul.ac.uk

The online version of this article contains supplemental material.

Abbreviations used in this article: Ct, cycle threshold; Gal-3, galectin-3; i.s., intrascrotal; KC, keratinocyte-derived chemokine; KO, knockout; L-PHA, *Phaseolus vulgaris* leukoagglutinin; mEC, murine endothelial cell; MLEC, murine lung endothelial cell; rGAL-3, recombinant Gal-3; WT, wild-type.

Materials and Methods

Animals

Breeding founders for the Gal-3$^{-/-}$ mouse colony were obtained from the Consortium for Functional Glycomics on a C57BL/6 background, and a colony was established at Charles River U.K. Male mice bearing GFP under their CX3/CR1 promoter were kindly donated by Prof. S. Nourshargh at the Centre for Microvascular Research, Queen Mary University of London (London, U.K.). In all experiments, age- and sex-matched controls (wild-type [WT] C57BL/6) were also purchased from Charles River U.K. All animals were fed standard laboratory chow and water ad libitum and were housed in a 12-h light–dark cycle under specific pathogen-free conditions. All experiments were performed with mice (20–28 g), strictly following U.K. Home Office regulations (Guidance on the Operation of Animals, Scientific Procedures Act, 1986).

Reagents

Recombinant mouse IL-1β and TNF-α and Power SYBR Green Mastermix were purchased from Thermo Fisher Scientific (Waltham, MA). PE-conjugated anti-mouse Ly6g (clone 1A8) and FITC-conjugated Ly-6G were purchased from BD Pharmingen. PE-conjugated Gal-3 (clone M3/83), PE-conjugated IgG2a isotype control (clone eBR2a), PE-conjugated CD11b (clone M1/70), allophycocyanin-conjugated L-selectin (CD62L) (clone MEL-14), allophycocyanin-conjugated IgG2a κ and PE-conjugated IgG2b k isotype controls, murine FC block, and multi species 10× RBC lysis buffer were all purchased from eBioscience (Hatfield, U.K.). Alexa Fluor 488 Ly-6C (clone HK1.4) and Pacific Blue–conjugated Ly-6G (clone 1A8) were from BioLegend (Cambridge, U.K.). Streptavidin PE-conjugated secondary Ab was from Invitrogen (Paisley, U.K.). Alexa Fluor 488–conjugated fibrinogen was from Fisher Scientific (Loughborough, U.K.). Recombinant mouse E-selectin Fc Chimera, recombinant mouse ICAM-1 Fc Chimera, and the mouse cytokine array panel A Proteome Profiler were from R&D Systems (Abingdon, U.K.). Alexa Fluor 555–conjugated VE-Cadherin and Alexa Fluor 647–conjugated MRP14 were kindly supplied by S.N. Histopaque 1119 and 1077 were from Sigma-Aldrich (Dorset, U.K.). Recombinant Gal-3 (rGal-3) was kindly supplied by GalPharma (Japan). The following lectins were purchased from Vector Laboratories (Peterborough, U.K.): HPA, SNA, PNA, MAL II, and *Phaseolus vulgaris* leukoagglutinin (L-PHA).

Intravital microscopy

Intravital microscopy of the cremaster muscle was carried out as previously described (12). Male mice were anesthetized with Isoflurane gas before an intrascrotal (i.s.) injection of PBS (sham), IL-1β (30 ng), TNF-α (300 ng), or Gal-3 (200–1000 ng) in a final volume of 400 μl. The injection was carried out 2 or 4 h before the vessel was recorded, allowing time for the 30-min stabilization period after the surgery had been completed. Before the i.s. injection, some animals also underwent a tail-vein i.v. injection of fluorescent Ab, rat anti-mouse Ly-6G (2 μg) in 200 μl saline. In brief, mice were anesthetized using a mixture of xylazine (7.5 mg/kg; Rompun) and ketamine (150 mg/kg; Narketan) by i.p. injection. The cremaster muscle was exteriorized and secured over the viewing stage; throughout the recordings it was superfused with bicarbonate buffered solution held at 37°C. Brightfield recordings were carried out using a Zeiss Axioskop FS microscope (Carl Zeiss). Fluorescence microscopy was carried out using an Olympus BX61W1 microscope (Carl Zeiss) connected to an Olympus BXUCB lamp, Uniblitz VCMD1 shutter driver, and DG4-700 shutter instrument, and recordings were captured using Slidebook 5.0 software (Intelligent Imaging TTL). An Optical Doppler Velocimeter (Microvascular Research Institute, Texas A&M University) was used to ensure that centerline RBC velocity remained adequate. Vessel segments of 100 μm in postcapillary venules with a diameter of 20–40 μm, an adequate centerline velocity (≥500 s^{-1}), and no branches within 100 μm of either side of the segment to be analyzed were chosen. Leukocyte rolling velocity (μm/s), adhesion (>30 s stationary), and emigration (50 μm by 100 μm either side of the vessel) were quantified.

Ex vivo flow chamber assay

This assay was used to assess leukocyte behavior under conditions of flow, which were generated using an automated syringe pump (Harvard Apparatus) connected to small-diameter tubing and chamber slides, allowing observation of the leukocytes over a layer of recombinant E-selectin. Ibidi μ-Slide VI0.4 cell microscopy chambers were coated with recombinant mouse E-selectin Fc Chimera (2 μg/ml) in 100 μl PBS/well for 2 h at room temperature. The wells were blocked using 0.5% Tween 20 in PBS for 1 h at room temperature. Murine whole blood was collected by cardiac puncture, diluted 1:10 in HBSS, and flowed through the chamber at 1.010 ml/min for 3 min. This was followed by HBSS at the same rate for 1 min before image acquisition and subsequent offline analysis. In some experiments, the whole blood was pretreated for 15 min at 37°C with rGal-3 (10 ng/ml) prior to flow. The flow chamber slides were viewed using a Nikon Eclipse TE3000 and six 10-s frames were collected for each well using a Q-Imaging Retiga EXi Digital Video Camera (Q-Imaging); recordings were analyzed using Image Pro-Plus software (Media Cybernetics).

In a further series of experiments, crawling of bone marrow leukocytes on ICAM-1 was assessed. Cells were isolated from the tibias and femurs of mice as described previously (13). In brief, bones were flushed with RPMI 1640 containing 10% FCS and 2 mM EDTA, and the resulting cell suspension was passed through a 100-μm filter. After hypotonic lysis of RBCs with 0.2% NaCl, cells were washed in RPMI 1640 and resuspended in 1 ml of ice-cold PBS. Cells were layered onto a double density gradient of Histopaque and centrifuged for 30 min at 2000 rpm without brake. Neutrophils were then collected from the interface between the 1119 and 1077 Histopaque layers, counted, and resuspended at 1×10^6/ml. Ibidi chamber slides were coated with recombinant mouse ICAM-1 Fc Chimera (2.5 μg/ml). Bone marrow neutrophils were stimulated with TNF-α (10 ng/ml) and allowed to adhere within the chamber for 5 min. HBSS was then flowed through the chamber at 2 dyne/cm^2, and frames were recorded every 10 s for 15 min as described earlier. Cell crawling was analyzed using the cell-tracking function in ImageJ software, and tracks were analyzed utilizing Ibidi Chemotaxis and Migration Tool. Only cells that started and remained within the field of view over the entire course of video capture were analyzed. At least 45 cells were tracked per mouse.

Analysis of leukocyte glycosylation profile, cell adhesion molecule expression, and integrin activation

Gal-3$^{-/-}$ or WT mice were deeply anesthetized, and up to 900 μl of blood was collected by cardiac puncture into heparin-coated syringes (100 μl of 100 U/ml). Murine whole blood was treated for 15 min at 37°C with PBS (sham), murine IL-1β (1–100 ng/ml), or murine TNF-α (10–200 ng/ml) before centrifuging at 300 × *g* for 5 min and aspiration of the supernatant. Cells were resuspended in murine FC Block (0.5 μg/ml) and incubated for 10 min on ice. The following rat anti-mouse primary Abs were added directly to the wells and incubated for 45 min on ice in the dark: PE-conjugated Gal-3 (8 μg/ml), PE-conjugated IgG2a isotype control (8 μg/ml), FITC-conjugated Ly-6G (5 μg/ml), PE-conjugated CD11b (2 μg/ml), PE-conjugated IgG2b k (2 μg/ml), allophycocyanin-conjugated L-selectin (1 μg/ml), allophycocyanin-conjugated IgG2a κ (1 μg/ml), and Alexa Fluor 488 Ly-6C (2.5 μg/ml). RBCs were lysed with multispecies lysis buffer, and the plate was washed twice in PBS-BSA before samples were transferred to flow cytometry tubes in 2% PFA and analyzed on a FACSCalibur (BD Biosciences).

To assess CD11b activation, we stimulated bone marrow neutrophils with fMLF (1 μM) or PMA (50 ng/ml) for 15 min in the presence of Alexa Fluor–conjugated fibrinogen (250 μg/ml). Neutrophils were subsequently labeled with Pacific Blue–conjugated Ly-6G (1.25 μg/ml), and fibrinogen binding on the Ly-6G$^+$ population was assessed on a BD LSRFortessa.

For the lectin binding assay, murine whole blood immediately underwent red cell lysis and following this were incubated with FC Block (0.5 μg/ml) for 10 min before the addition of the following Abs and biotinylated lectins for 45 min at room temperature: FITC-conjugated Ly-6G (5 μg/ml), Alexa Fluor 488 Ly-6C (2.5 μg/ml), HPA (20 μg/ml), SNA (166 ng/ml), PNA (20 μg/ml), MAL II (3.3 μg/ml), and L-PHA (4 μg/ml; Vector Laboratories). The cells underwent incubation for 30 min at room temperature with a streptavidin PE-conjugated secondary Ab (120 ng/ml in PBS-BSA) and fixation in 2% PFA before analysis on a FACSCalibur.

Isolation of murine lung endothelial cells

Murine lung endothelial cells (MLECs) were isolated from the lungs of Gal-3$^{-/-}$ or WT mice as described previously (14). In brief, lungs were excised and placed in Ham's F12 media (Life Technologies) on ice. After maceration, the tissue was further digested in 10 ml 1 mg/ml collagenase Type I-S for 2 h at 37°C. The digest was diluted in 10 ml MLEC media (equal parts low-glucose DMEM and Ham's F12 [Life Technologies] containing heparin [100 μg/ml; Sigma], penicillin [100 U/ml], streptomycin [100 μg/ml] and L-glutamine [2 mM; Sigma], endothelial cell growth supplement [25 μg; AbD Serotec] and 20% FCS) and passed through a 19.5-gauge needle followed by a 70-μm cell strainer (BD Falcon). The resulting cell suspension was cultured in flasks precoated with 10 ml 0.1% gelatin in PBS containing bovine collagen (30 μg/ml, 97% type I, 3% type III; Nutacon) and bovine plasma fibronectin (10 μg/ml; Sigma).

Endothelial cells were first purified by removal of contaminating macrophages using Dynabeads (10 μl/3 ml; Dynal Biotech) and a rat anti-mouse CD16/32 (5 μg/3 ml; BD Biosciences) Ab. Sorted cells were then cultured until colonies of ~20 endothelial cells could be seen.

The culture was purified further by positive selection for the endothelial cells using ICAM-2/CD102 [clone 3C4(mIC2/4), 10 μg/3 ml; BD Pharmingen]. Ten milliliters of MLEC media was used to resuspend the cells, which were then cultured until they reached 50% confluence, at which point the positive sort was repeated to enhance the culture.

Analysis of murine endothelial cell adhesion molecule expression

WT and Gal-3$^{-/-}$ MLECs were treated for 4 h with PBS (sham) or murine IL-1β (1–100 ng/ml) and then detached using Accutase. Cells were incubated with murine Fc Block (0.5 μg/ml; eBioscience). The following rat anti-mouse primary Abs were added directly to the cells with Fc Block and incubated on ice: PE-conjugated CD31 (clone MEC 13.3, 4 μg/ml; BD Pharmingen), PE-conjugated CD54 (clone YN1/1.7.4, 2 μg/ml; eBioscience), PE-conjugated IgG2bκ (2 μg/ml; eBioscience), FITC-conjugated CD102 (clone 3C4, 10 μg/ml; BD Pharmingen), purified CD62E (clone 10E9.6, 5 μg/ml; BD Pharmingen). Cells were washed twice in PBS-BSA and transferred to flow cytometry tubes in 2% PFA before analysis on a FACSCalibur.

Ex vivo confocal microscopy of the cremaster

Cremasters from CX3/CR1 GFP mice were exteriorized and fixed in 4% PFA before permeabilization and blocking in PBS containing 12.5% each of FBS and normal goat serum and 0.5% Triton X-100 for 2 h at room temperature. Primary Abs against VE-Cadherin (Alexa Fluor 555 conjugated) and MRP14 (Alexa Fluor 647 conjugated) were applied overnight at 4°C, and the vessels were viewed using a Leica SP5 confocal microscope using a resonance scanner of 8000 Hz.

Assessment of murine cremaster mRNA

Murine cremaster muscles were dissected and snap frozen in LN_2 before tissue disruption using the Precellys 24 tissue homogenizer (5500 × *g*, 3 × 20 s). The supernatant was further disrupted by passage through a 27-gauge syringe before RNA isolation with the RNeasy kit and on-column DNase. RNA was reverse transcribed into cDNA. Quantitative real-time PCR was performed using Power SYBR Green Mastermix (Applied Biosystems). Primers included those for Lgals3, Gapdh, Rpl32, Il-1b, tnf, Il-6, Ccl2, Cxcl1, Cxcl12, Ly-6G, Csf1r, Pecam1, Icam1, and Sele. Thermal cycling was carried out using the ABI Prism 7900 Real Time PCR system according to manufacturer recommendations. The comparative cycle threshold (Ct) method (15) was used to measure gene transcription, where the Ct values were first normalized with an endogenous housekeeping gene and then to the control samples, which were used as a calibrator and given a value of 1, and the results were expressed as relative units based on $2^{-\Delta\Delta Ct}$.

Protein expression of cytokines and chemokines in the cremaster

Murine cremaster muscles were dissected and snap frozen in LN_2 before disruption in 600 μl of PBS containing protease inhibitors aprotinin, leupeptin, and pepstatin (all 10 μg/ml) using the Precellys 24 tissue homogenizer (600 × *g*, 2 × 30 s). The supernatant was collected and 1% Triton X-100 was added before the samples underwent freezing at −80°C. After thawing, the samples were centrifuged at 10,000 × *g* for 5 min. A final protein quantity of 200 μg was then assessed using the mouse cytokine array panel A Proteome Profiler according to the manufacturer's instructions.

Statistical analysis

All data were analyzed using GraphPad Prism 4 software. Data are expressed as mean ± SEM of *n* experiments. All data were tested for normal distribution. Statistical significance was assessed using unpaired Student *t* tests, one-way ANOVA, or two-way ANOVA with the appropriate post hoc test, commonly Dunnett posttest or the Tukey range test. In all cases, $p \leq 0.05$ was considered significant.

Results

Endogenous Gal-3 is required for reduction in leukocyte rolling velocity in response to TNF-α and IL-1β, and leukocyte emigration in response to IL-1β, in inflamed postcapillary venules

The cremasteric microcirculation of Gal-3$^{-/-}$ mice was assessed after 4-h treatment with TNF-α (300 ng) or IL-1β (30 ng), reflecting the time taken to see significant changes in leukocyte recruitment in WT mice (Fig. 1A–C). It is well established that these two stimuli are important proinflammatory modulators of the acute inflammatory response (16, 17), as well as in chronic pathologies, for example, rheumatoid arthritis (18, 19). The administration of these cytokines in vivo results in leukocyte recruitment that may differ in mode; for example, an early study examining responses to both cytokines intradermally in the rabbit found that IL-1β–induced neutrophil extravasation peaked at 3–4 h, whereas TNF-α–induced neutrophil extravasation was much quicker and also associated with protein synthesis-independent edema formation (20). After TNF-α treatment, Gal-3$^{-/-}$ mice displayed similar levels of leukocyte adhesion (Fig. 1B, 1D) and emigration (Fig. 1C, 1D); however, they lacked the reduction in rolling velocity observed in WT animals that is characteristic of E-selectin–dependent rolling (Fig. 1A) (21). A similar observation was made in mice treated with IL-1β (30 ng), where average rolling velocity was reduced in WT mice, but not in Gal-3$^{-/-}$ animals (Fig. 1A). In addition, significantly fewer leukocytes emigrated in Gal-3$^{-/-}$ mice after IL-1β treatment when compared with WT animals, a reduction that was not observed in response to TNF-α (Fig. 1C).

Leukocyte binding to E-selectin and subsequent cellular morphological changes are disrupted in the absence of endogenous Gal-3

Because leukocyte rolling is dependent on selectin binding, with slow rolling predominantly mediated by E-selectin in this model (21), we next examined the role of Gal-3 in E-selectin–dependent rolling in greater depth. Experiments were performed under flow whereby whole blood from C57BL/6 or Gal-3$^{-/-}$ mice was flown through chambers coated with recombinant E-selectin. We show that under conditions of flow, Gal-3$^{-/-}$ leukocytes exhibit a reduced capacity to adhere to E-selectin when compared with WT cells (Fig. 2A). Additionally, two types of leukocyte behaviors were observed; some cells remained phase bright, whereas some leukocytes displayed a more active phenotype and changed their morphology to become phase dark (Fig. 2C), likely because of E-selectin ligation, which initiates intracellular signaling pathways leading to neutrophil activation (22). We found that a smaller proportion (percentage of total cells) of Gal-3$^{-/-}$ cells displayed phase dark morphology when compared with WT cells (Fig. 2B). This phenotype was not rescued by the addition of plasma levels (10 ng/ml, as assessed by ELISA) of rGal-3 to Gal-3$^{-/-}$ blood (Fig. 2D). Importantly, there was no significant difference in WBC count (cells per microliter) between WT and Gal-3$^{-/-}$ mice (WT 29.92 ± 0.17 versus knockout [KO] 28.00 ± 3.41, NS); consequently, any differences observed can be attributed to changes in the leukocytes themselves. This is in line with full hematological reports published by the Consortium for Functional Genomics, which find no differences in Gal-3$^{-/-}$ leukocyte cell counts when compared with WT mice (23). These results suggest that, in the absence of Gal-3, the cells lack the machinery needed to bind E-selectin and facilitate the downstream signaling pathways that are initiated once bound; thus, E-selectin ligands were studied in greater depth.

Murine neutrophils display reduced PNA and HPA lectin binding sites on their cell surface

Because there have been no reports of direct interactions between galectins and selectins, we hypothesized that lack of endogenous Gal-3 may affect the availability of selectin ligands. All selectin ligands carry sLe^x, commonly on α1,3-fucosylated and α2,3-sialylated *O*-glycans; although they are less well understood, E-selectin ligands

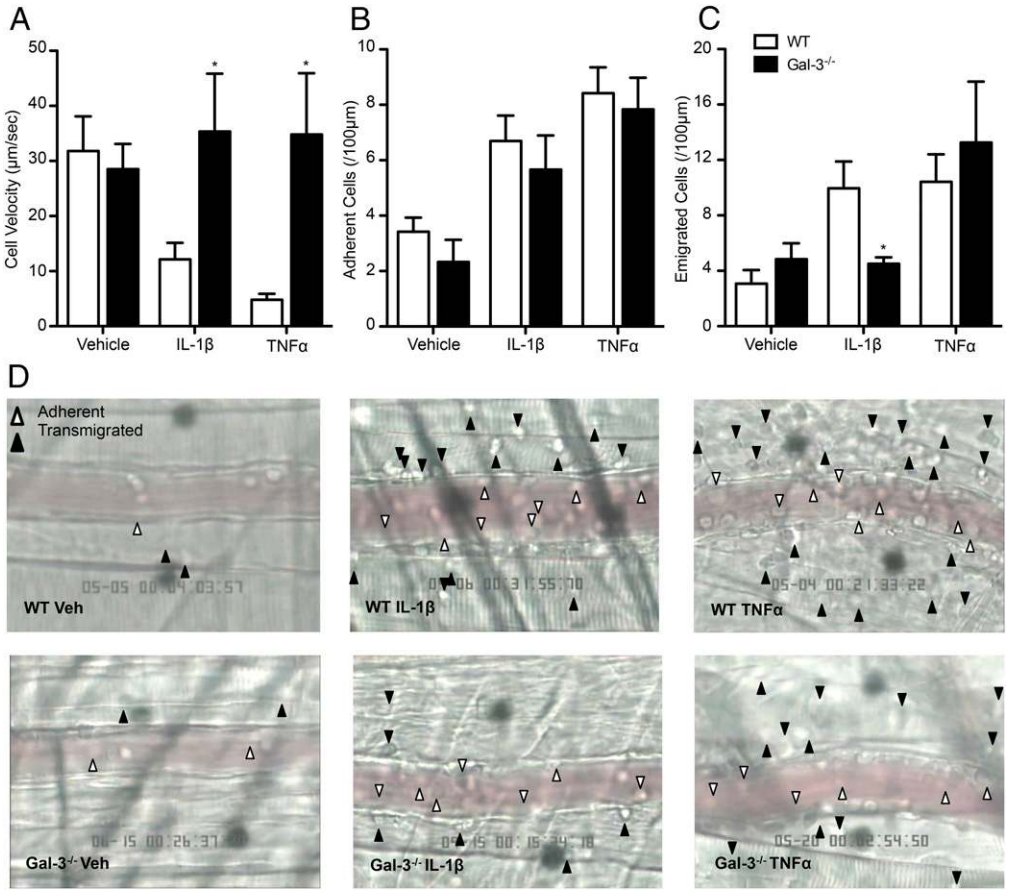

FIGURE 1. Endogenous Gal-3 is required for leukocyte slow rolling in response to TNF-α and IL-1β and leukocyte emigration in response to IL-1β in postcapillary venules. Cremasteric postcapillary venules of C57BL/6 or Gal-3$^{-/-}$ mice were analyzed by intravital microscopy after i.s. injection of TNF-α (300 ng) or IL-1β (30 ng) 4 h before exteriorization. (**A**) Leukocyte rolling velocity. (**B**) Number of adherent leukocytes (>30 s). (**C**) Number of emigrated leukocytes. All data were obtained from segments of 100 μm in three to five vessels per mouse and three to five mice per group. Results are expressed as mean ± SEM for all parameters analyzed. Statistical significance was assessed by two-way ANOVA and with Bonferroni multiple comparison posttest. *$p < 0.05$. (**D**) Representative images from vessels of C57BL/6 (upper panel), or Gal-3$^{-/-}$ mice (lower panel) after vehicle, IL-1β, or TNF-α treatment show rolling, adherent, and emigrated leukocytes.

specifically must be modified by a fucosyltransferase such as fucosyltransferase VII or IV to be functional. Hence the glycosylation pattern of Gal-3$^{-/-}$ leukocytes was assessed, because any inherent changes would greatly affect the ability of E-selectin ligands such as ESL-1, PSGL-1, and CD44 to bind. Because untreated Gal-3$^{-/-}$ leukocytes exhibited reduced capture to E-selectin under conditions of flow, basal levels of lectin binding by neutrophils were analyzed by flow cytometry. This was carried out using cell markers and a panel of biotinylated lectins, which each bind glycans of different structures. When compared with their WT counterparts, Gal-3$^{-/-}$ neutrophils were found to display comparable binding of the lectins SNA, L-PHA, and MAL II, but presented a marked reduction in binding of PNA and HPA (Fig. 3).

Cells lacking endogenous Gal-3 display altered ligand expression in response to IL-1 β and TNF-α

We previously observed that endogenous Gal-3 is required for complete leukocyte emigration in response to IL-1β, but not TNF-α. These two classical stimuli are known to have differing and cell type–specific roles; IL-1β activates the endothelia directly, whereas WT neutrophils respond to TNF-α by increasing their expression of β_2-integrin (CD18) and shedding L-selectin (24). We therefore assessed the effects of these two stimuli on adhesion molecule expression of WT and Gal-3$^{-/-}$ leukocytes (Fig. 4).

WT or Gal-3$^{-/-}$ whole blood was treated for 10 min at 37°C with vehicle (PBS), TNF-α (50 ng/ml), or IL-1β (50 ng/ml) before cell staining with Abs against CD11b and L-selectin, as well as the neutrophil marker Ly-6G (clone 1A8). In contrast with treatment with IL-1β, which did not alter expression from vehicle-treated cell levels, treatment with TNF-α increased neutrophil expression of CD11b in WT cells (Fig. 4A). Furthermore, when compared with their WT counterparts, Gal-3$^{-/-}$ neutrophils exhibited significantly reduced levels of CD11b basally and after cytokine treatment (Fig. 4A). To assess whether CD11b activation is also reduced in Gal-3$^{-/-}$ neutrophils, we measured binding of Alexa488-conjugated fibrinogen to bone marrow–derived neutrophils from Gal-3$^{-/-}$ and WT mice. Stimulation of neutrophils with PMA (50 ng/ml) significantly increased fibrinogen binding to both Gal-3$^{-/-}$ and WT neutrophils compared with untreated cells; however, fibrinogen binding was not significantly different between the two genotypes (Supplemental Fig. 1A). In line with a lack of difference in CD11b activation between the two genotypes, there was no difference in neutrophil crawling (distance traveled or crawling velocity) on rICAM-1 between TNF-α–stimulated bone marrow neutrophils from Gal-3$^{-/-}$ or WT mice (Supplemental Fig. 1B, 1C). In a similar fashion to CD11b expression patterns in WT neutrophils, treatment with TNF-α induced L-selectin shedding, although IL-1β did not (Fig. 4C). However, L-selectin shedding was unaltered in the Gal-3$^{-/-}$ neutrophils basally and after TNF-α treatment (Fig. 4C).

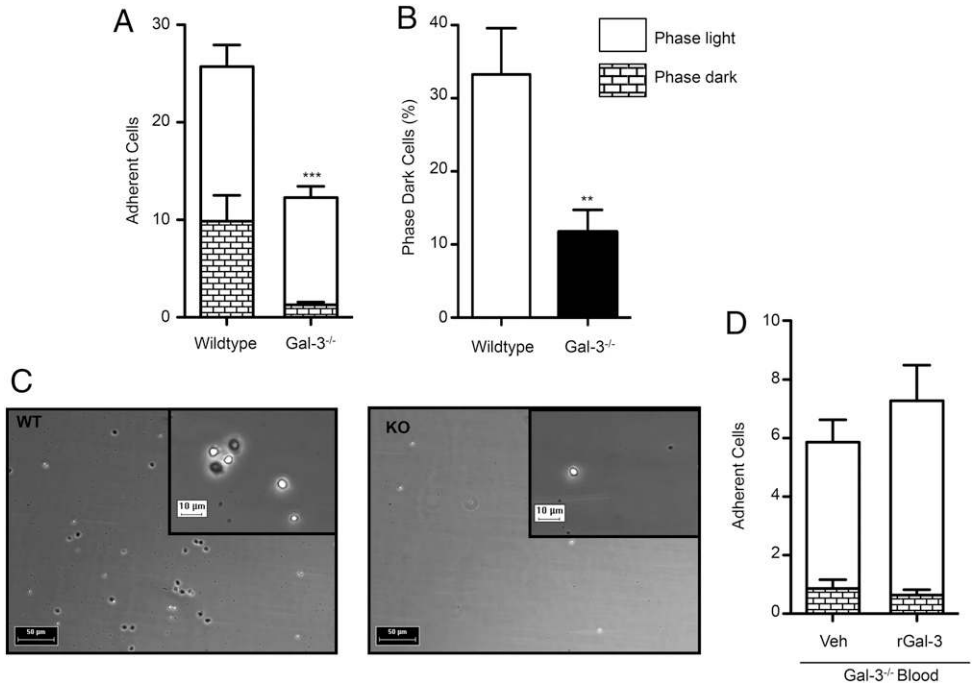

FIGURE 2. Leukocyte binding to E-selectin and subsequent cellular morphological changes are disrupted in the absence of endogenous Gal-3. Murine leukocyte interactions with recombinant E-selectin were examined under conditions of flow. C57BL/6 or Gal-$3^{-/-}$ whole blood was collected by cardiac puncture and diluted in HBSS. Blood was flown for 3 min at 1.010 ml/min, followed by 1 min HBSS. Videos of 10 s were captured for a total of four to six frames per mouse and three mice per group. Captured leukocytes in each frame were quantified and classified as phase dark or phase light according to their cellular morphology. The number of adherent cells was quantified (**A**), and the percentage of cells transitioning to phase dark was calculated for each genotype (**B**). (**C**) Representative stills taken from C57BL/6 (left panel) or Gal-$3^{-/-}$ (right panel) experiments. Scale bars, 50 μm; higher magnification shown in inset, scale bars, 10 μm. (**D**) Gal-$3^{-/-}$ whole blood was pretreated for 15 min at 37°C with rGal-3 (10 ng/ml) prior to flow. Results are expressed as mean ± SEM. Significance was assessed using an unpaired Student *t* test. $^{**}p < 0.01$, $^{***}p < 0.001$.

To examine the direct effects of IL-1β on the endothelium, we treated confluent WT and Gal-$3^{-/-}$ murine endothelial cells (mECs) for 4 h with the cytokine (1–100 ng/ml). ICAM-1 and E-selectin expression levels were then quantified by flow cytometry. When compared with their WT counterparts, Gal-$3^{-/-}$ mECs expressed reduced E-selectin and ICAM-1 on their surface after IL-1β treatment (Fig. 4E, 4F).

Administration of exogenous Gal-3 results in neutrophil and monocyte recruitment to postcapillary venules

In addition to its intracellular localization, Gal-3 is secreted and found extracellularly, where it exerts its effects predominantly by interacting with glycans on the cell surface and associated with the extracellular matrix. To establish whether exogenous Gal-3 is capable of initiating leukocyte recruitment to the cremasteric microcirculation in the absence of a classical inflammagen, we conducted a time course using rGal-3. Intravital microscopy was first performed using WT C57BL/6 mice, which were injected i.s. with rGal-3 (500 ng) 2 or 4 h before subsequent analysis (Fig. 5). Leukocyte recruitment overall was increased at the 4-h, but not the 2-h, time point with no significant differences observed between sham-treated animals and those treated with Gal-3 for 2 h (Fig. 5A). In comparison, at 4 h, the microcirculation displayed significantly reduced leukocyte rolling velocities, as well as significant increases in both adhesion and emigration (Fig. 5A). Once we had established that Gal-3 could elicit an inflammatory response, we were interested to establish whether the lectin would act dose-dependently and exhibit cell type–specific responses.

After Ab validation, murine anti–Ly-6G was used to label neutrophils recruited to the cremaster in C57BL/6 mice treated with rGal-3 (200–1000 ng in 400 μl PBS i.s.). Rolling velocities were significantly reduced from sham levels in both 500 and 1000 ng treated mice, and this reduction was similar for Ly-6G −ve and Ly-6G +ve cells (Fig. 5B). After 1000 ng rGal-3 treatment, levels of both adherent and emigrated cells were significantly increased from sham for both Ly-6G −ve and Ly-6G +ve cells (Fig. 5B). This confirms that in this system exogenous Gal-3 can act specifically to increase neutrophil trafficking to the inflamed area in vivo; however, approximately half of the recruited cells remained unidentified. To investigate monocyte recruitment in isolation, we assessed the cremasteric microcirculation in $CX_3CR1^{gfp/+}$ mice 4 h after i.s. injection of PBS (sham) or rGal-3 (1000 ng). Monocyte rolling velocity was significantly reduced after rGal-3 treatment (Fig. 5D). This was in addition to increased adhesion and emigration of monocytes to the inflamed rGal-3–treated area (Fig. 5D). These results were confirmed using cremaster muscles from rGal-3–treated (1000 ng) $CX_3CR1^{gfp/+}$ mice, which were exteriorized and stained using Abs against VE-cadherin and MRP14 (Fig. 5F). Similarly to the vessels analyzed by intravital microscopy, mice treated with rGal-3 exhibited increased emigration of both neutrophils and monocytes when compared with sham-treated animals, and these cell types were present in the tissue in an approximate ratio of 50:50 (Fig. 5G).

Exogenous Gal-3 treatment results in increased proinflammatory cytokine and chemokine expression in the local tissue microenvironment

To further examine the effects of rGal-3 on the tissue after i.s. injection, we conducted real-time PCR analysis of expression of various inflammatory genes. The cremasters from C57BL/6 mice treated i.s. with vehicle control (PBS) or rGal-3 (1000 ng) were analyzed. When compared with their sham-treated counterparts,

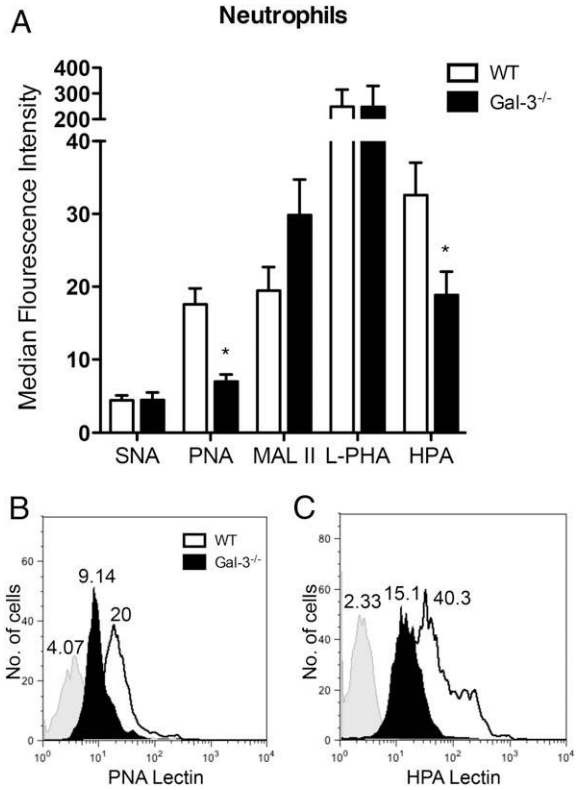

FIGURE 3. Murine neutrophils display reduced PNA and HPA lectin binding sites on their cell surface. WT or Gal-3$^{-/-}$ whole blood was collected by cardiac puncture before analysis by flow cytometry. (**A**) Ly-6G^{+} neutrophils were assessed for their ability to bind the lectins SNA, PNA, MAL II, L-PHA, and HPA by flow cytometry. (**B**) Representative histogram plot showing PNA lectin binding on WT and Gal-3$^{-/-}$ neutrophils, with isotype control (gray). (**C**) Representative histogram plot showing HPA lectin binding on WT and Gal-3$^{-/-}$ neutrophils, with isotype control (gray). Results are expressed as mean ± SEM of three to six mice per group. Significance was assessed using an unpaired Student *t* test. *$p < 0.05$.

cremaster muscle treated with rGal-3 displayed significantly increased mRNA for *Il1b*, *Cxcl1*, *Ccl2*, and *Il6*, and there was a trend for increased TNF-α (Fig. 6A). In contrast, the expression of *Cxcl12* was not changed in rGal-3–treated cremaster muscle when compared with sham preparations.

To confirm that this increase in proinflammatory gene expression results in increased protein, we dissected murine cremaster muscles after i.s. treatment with rGal-3 (1000 ng) for 4 h. Frozen cremasters were homogenized, and a final protein quantity of 200 μg was then assessed using the mouse cytokine array panel A Proteome Profiler. The proteome array of rGal-3–treated cremaster samples displayed increased binding of many cytokines and chemokines, when compared with sham cremaster arrays (Fig. 6B). Cytokines increased after rGal-3 treatment included IFN-γ, MCP-1 (CCL2), IL-6, keratinocyte-derived chemokine (KC; CXCL1), MIP-1α (CCL3), MIP-2 (CXCL2), and TNF-α. Crucially, these effects were not unidirectional, and levels of some proteins in rGal-3–treated arrays were comparable or reduced when compared with control arrays, for example, MIP-1β and BCA-1.

Administration of rGal-3 i.v. does not affect leukocyte recruitment or cell adhesion molecule expression

Despite treating locally with rGal-3, we wanted to ensure that the lectin was not entering the systemic circulation and acting on neutrophils and monocytes directly. Of note here are previous studies suggesting that Gal-3 may act as a soluble adhesion molecule for neutrophils in vitro, where it increased their binding to endothelial monolayers (11, 25). In addition, Gal-3 promotes human neutrophil adherence to the extracellular matrix proteins laminin and fibronectin. This effect is dependent on the carbohydrate recognition domain and amino terminal of Gal-3, as well as being temperature and Ca^{2+}/Mg^{2+} dependent, suggesting that Gal-3 oligomerizes at the cell surface (25). Furthermore, when the two cell types are incubated together in vitro, Gal-3 forms clusters between the endothelial cell surface and adherent neutrophils; these are concentrated at tricellular corners of the endothelium, where these cells preferentially transmigrate (26). The cremasteric microcirculation was therefore assessed after i.v. administration of vehicle (saline, 200 μl) or rGal-3 (150 ng). It was found that administration of rGal-3 had no effect on leukocyte recruitment to the area over a 60-min period, suggesting that exogenous Gal-3 does not act on leukocytes or vascular endothelial cells directly, at least within 60 min (Supplemental Fig. 2A–D). Furthermore, analysis of leukocytes by flow cytometry after i.v. administration of rGal-3 revealed that the expression of cell adhesion molecules such as PSGL-1, L-selectin, CD44, or CD11a, CD11b, and CD11c was unchanged in response to this lectin (Supplemental Fig. 2E). These results reflect those seen in the ex vivo flow chamber (Fig. 2D), where rGal-3 did not affect interactions of leukocytes with E-selectin in isolation (Fig. 7).

Discussion

The goal of this study was to investigate whether Gal-3 acted as a positive regulator of leukocyte recruitment in vivo. The results reveal previously unreported roles for Gal-3 in controlling the dynamics of vascular leukocyte recruitment. We have shown that adhesion molecule expression is compromised in the absence of Gal-3, leading to reduced leukocyte trafficking in vivo and adhesion/activation in vitro. A prorecruitment role for Gal-3 is further evidenced by the ability of the recombinant protein to induce the generation of multiple soluble proinflammatory mediators and to enhance leukocyte transmigration. Overall, these results suggest that Gal-3 is required for the efficient recruitment of leukocytes during an acute inflammatory response.

The actions of galectins are complex and depend on their cellular localization, with intracellular functions often at odds with their effects once released in the extracellular environment. This is the case for Gal-3, because the intracellular protein can inhibit T cell apoptosis (27), whereas extracellular Gal-3 induces apoptosis (28). It is also apparent that the actions of Gal-3 are stimulus specific, particularly when considering its role in neutrophil trafficking (11, 29, 30). Although previous studies suggest that Gal-3 facilitates leukocyte recruitment and may even function as an adhesion molecule when it is present in inflammatory exudates (11), its actions on the leukocyte recruitment cascade have not been detailed. We have therefore addressed the roles of both the endogenous and the recombinant protein on the inflammatory response initiated by two major proinflammatory cytokines.

The data presented show that endogenous Gal-3 is required for slow rolling of leukocytes in response to local treatment with the proinflammatory cytokines IL-1β and TNF-α. The response to these cytokines differed, however, in terms of the impact of Gal-3 on leukocyte emigration, providing further evidence of stimulus-specific roles for this lectin. The reduced leukocyte emigration we observed in Gal-3$^{-/-}$ mice is in keeping with published results. Reduced monocyte, macrophage, and neutrophil recruitment to the CNS occurs in a model of EAE (31), and despite conflicting reports using a thioglycollate broth model of peritonitis, reduced infiltration of neutrophils was observed at either day 1 or 4 after insult (32, 33). Farnworth et al. (34) reported that Gal-3$^{-/-}$ mice exhibited more severe lung injury associated with reduced neutrophil

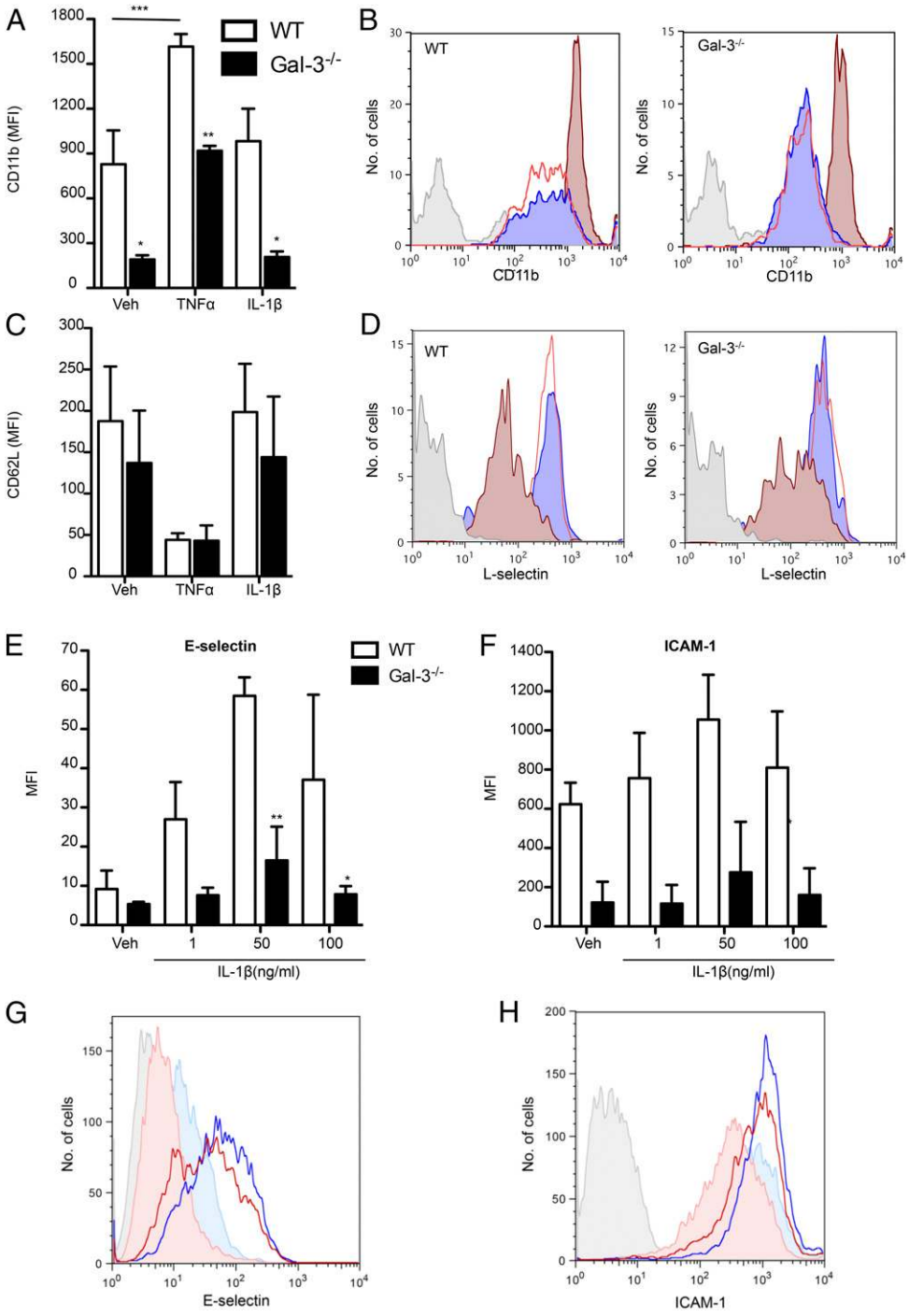

FIGURE 4. Cells lacking endogenous Gal-3 display altered ligand expression after activation with TNF-α and IL-1β. (**A**–**D**) WT or Gal-3$^{-/-}$ whole blood was treated for 10 min at 37°C with TNF-α (50 ng/ml) or IL-1β (50 ng/ml) and CD11b (A), and L-selectin (C) surface expression was assessed by flow cytometry. (B and D) Representative histogram plots of WT and Gal-3$^{-/-}$ neutrophils stained for isotype control (gray) or CD11b (B) or L-selectin (D) after treatment with vehicle (blue), IL-1β (red line), or TNF-α (dark red). (**E** and **F**) Confluent WT and Gal-3$^{-/-}$ mECs were treated for 4 h with IL-1β (1, 50, 100 ng/ml) before analysis by flow cytometry. Representative histogram plots showing isotype control (gray tinted), vehicle (PBS)-treated WT cells (filled pale blue), IL-1β (50 ng/ml)-treated WT cells (blue line), vehicle (PBS)-treated Gal-3$^{-/-}$ cells (filled pale red), and IL-1β (50 ng/ml)-treated Gal-3$^{-/-}$ cells (red line) stained for (**G**) E-selectin and (**H**) ICAM-1. Results are expressed as mean ± SEM of two to four mice per group, significance was assessed by two-way ANOVA and Bonferroni multiple comparison posttest. *$p < 0.05$, **$p < 0.01$, ***$p < 0.001$.

recruitment at 15 h after *Streptococcus pneumoniae* infection: of interest, neutrophil recruitment in this model is independent of β_2-integrins. This reduction in extravasated neutrophils at 12–24 h was also reported by Nieminen et al. (30), who found that recruitment was unaffected in β_2-integrin–dependent *Escherichia coli*–driven lung infection in Gal-3$^{-/-}$ animals. These studies have led to the hypothesis that Gal-3 may function as a bona fide adhesion molecule in response to particular stimuli. Our data suggest that, although this may be the case, with discrepancies between the response observed to IL-1β versus TNF-α, the role of Gal-3 extends beyond models in which the recruitment is β_2-integrin independent. The effects of Gal-3 on leukocyte recruitment we have identified in this study are not limited to neutrophils; Gal-3 expression is increased in murine lungs with

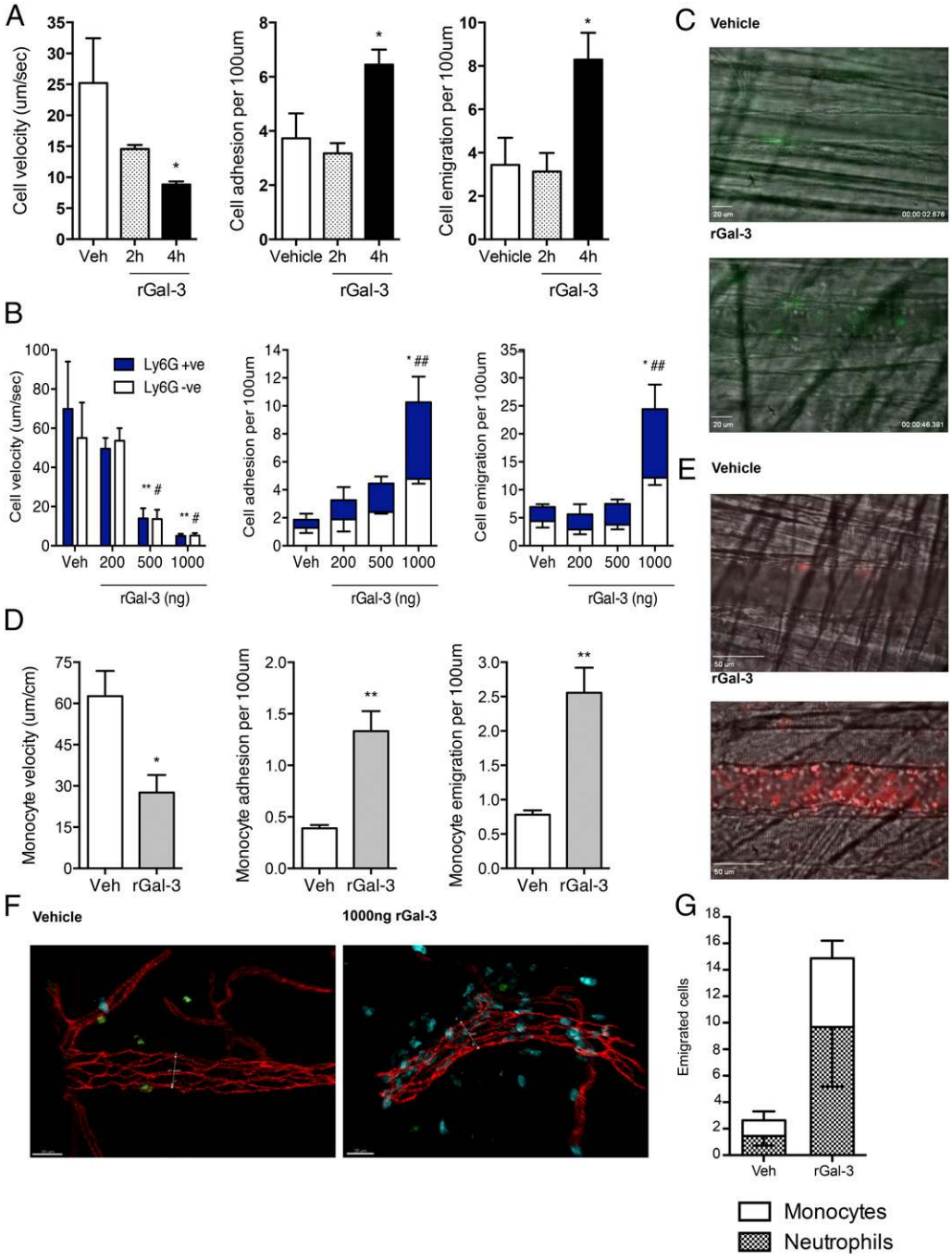

FIGURE 5. Administration of rGal-3 results in neutrophil and monocyte recruitment to postcapillary venules. Cremasteric postcapillary venules of C57BL/6 mice were analyzed by intravital microscopy after i.s. injection of rGal-3 (500 ng) 2 or 4 h before exteriorization. (**A**) Leukocyte rolling velocity, number of adherent leukocytes (>30 s), and number of emigrated leukocytes. Cremasteric postcapillary venules of $CX_3CR1^{gfp/+}$ mice were assessed 4 h after i.s. injection of rGal-3 (1000 ng), and GFP^+ monocyte rolling velocity, adhesion, and emigration were analyzed (**B**). (**C**) Representative images from vessels of $CX_3CR1^{gfp/+}$ mice after vehicle or rGal-3 administration, where monocytes are GFP^+ (green). (**D**) The cremasteric microcirculation in C57BL/6 mice was assessed 4 h after i.s. injection of rGal-3 (200–1000 ng) and i.v. administration of anti-mouse Ly-6G (2 μg) to label murine neutrophils. Ly-$6G^+$ cells are shown in the filled columns and Ly-$6G^-$ cells in the empty columns. (**E**) Representative images from vessels of C57BL/6 mice after vehicle or rGal-3 administration, where neutrophils are stained with anti-mouse Ly-6G (red). (**F**) Cremasters from $CX_3CR1^{gfp/+}$ mice treated intrascrotally for 4 h with rGal-3 (1000 ng) were exteriorized before analysis by confocal microscopy. Representative images from vehicle- and rGal-3–treated mice; vessels are stained using VE-cadherin (red), $MRP14^+$ neutrophils are blue, and GFP^+ monocytes are green. (**G**) Emigrated neutrophils and monocytes were quantified. All data were obtained from segments of 100 μm in three to five vessels per mouse and three to five mice per group. Results are expressed as mean ± SEM for all parameters analyzed. Scale bars, 20 μm (C and F), 50 μm (E). Statistical significance was assessed by one- or two-way ANOVA and with Tukey multiple comparison posttest or unpaired Student *t* tests. $^*p < 0.05$, $^{**}p < 0.01$, $^{\#}p < 0.05$, $^{\#\#}p < 0.01$ between Ly-6G +ve bars.

allergic asthma, and Gal-$3^{-/-}$ mice display reduced lung and airway eosinophilia in response to acute and chronic OVA challenge, respectively (35). Further investigation showed endogenous Gal-3 is required for rolling of bone marrow–derived eosinophils on VCAM-1 and showed a trend to be required for stable adhesion on ICAM-1 under conditions of flow. This was in addition to its requirement for subsequent activation-induced morphological changes such as cell spreading and protrusion

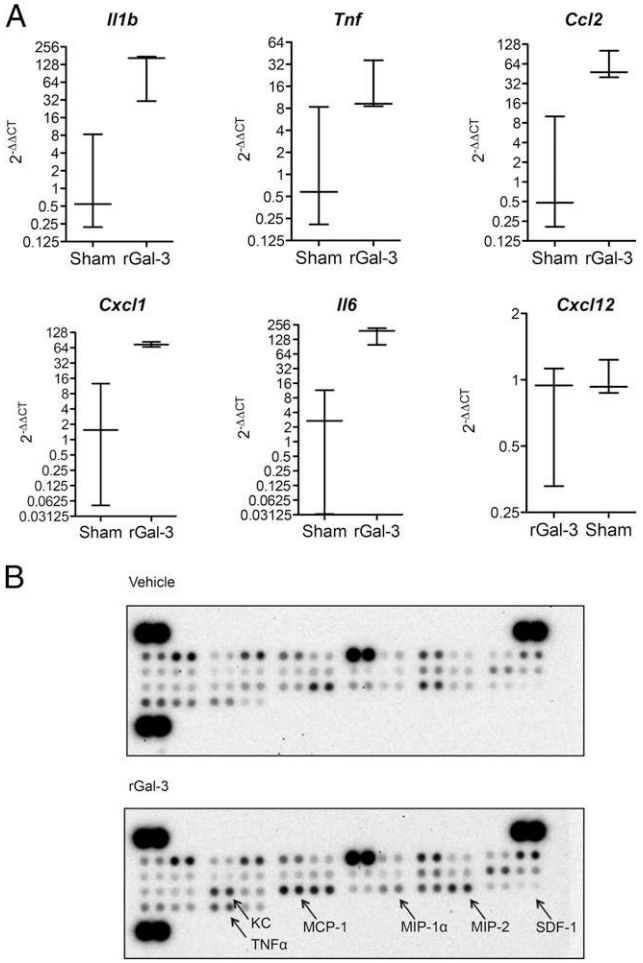

FIGURE 6. Administration of rGal-3 results in increased proinflammatory cytokine and chemokine expression in the local tissue microenvironment. The cremasteric tissue of C57BL/6 mice was assessed 4 h after i.s. injection of PBS or rGal-3 (1000 ng). (**A**) Gene expression of *Il1b*, *Tnf*, *Cxcl1*, *Ccl2*, *Il6*, and *Cxcl12* after exogenous Gal-3 treatment. Results are expressed as $2^{-\Delta\Delta Ct}$, where gene expression is normalized to an internal housekeeping gene (GAPDH) and then normalized once more to the sham cremasters. Results are displayed as mean ± SEM of two to three mice per group. (**B**) Protein content was assessed using the mouse cytokine array (A) Proteome Profiler using tissue homogenates from cremasters treated with exogenous Gal-3.

formation, as well as intracellular Gal-3 being vital for eosinophil migration to eotaxin-1 in Transwells (36).

Our findings suggest stimulus-specific roles for Gal-3 as evidenced by the different responses we observed to IL-1β and TNF-α in the absence of Gal-3. Because IL-1β activates the endothelia directly (24), the differences in leukocyte emigration quantified in Gal-$3^{-/-}$ mice suggest that endothelial function may be compromised in these animals, possibly in terms of their expression of cell adhesion molecules and junctional adhesion molecules involved in transmigration. Our finding that Gal-$3^{-/-}$ endothelial cells express reduced ICAM-1 and E-selectin after IL-1β treatment, an outcome that would have direct consequences for IL-1β–induced slow rolling and possibly subsequent transmigration, suggests that the function of the endothelium is defective in these mice. More recently, it was found that neutrophil transmigration elicited by IL-1β, but not TNF-α, is protein synthesis dependent and requires ICAM-2, JAM-A, then PECAM-1 in distinct but sequential steps (24, 37). In the future, the expression of these molecules in Gal-$3^{-/-}$ endothelial cells should be assessed, as well as their glycosylation pattern, because all three contain *N*-glycosylation sites (38–40). Also of interest to this study, IL-1β– but not TNF-α–induced neutrophil transmigration is dependent on α_6-integrin (41), which is recognized by HPA lectin, the binding of which was reduced in Gal-$3^{-/-}$ cells.

Furthermore, Young et al. (24) showed that WT neutrophils respond to TNF-α by increasing their expression of β_2-integrin (CD18) and shedding L-selectin, in contrast with cells treated with IL-1β. Because Gal-3 is not thought to affect β_2-integrin–dependent leukocyte recruitment (30), CD11b, which forms Mac-1 with the β_2-integrin CD18, was investigated. Flow cytometric analysis showed that Gal-$3^{-/-}$ neutrophils express reduced PSGL-1 in response to TNF-α, a finding that could have direct consequences for leukocyte slow rolling because PSGL-1 is a known ligand of E-selectin and these interactions support slow rolling in postcapillary venules (42). Also, Gal-$3^{-/-}$ neutrophils express reduced CD11b basally and after TNF-α treatment, although levels of L-selectin were comparable.

It is worth noting that despite this altered cell adhesion molecule expression on both Gal-$3^{-/-}$ neutrophils and endothelial cells, levels of adhesion were unchanged in Gal-$3^{-/-}$ mice, both basally and after stimulation. Kubes et al. (43) demonstrated that rolling needs to be reduced by ~90% to affect levels of leukocyte adhesion; these authors used a high dose of fucoidan, a sulfated homopolymer of fucose, to attain this level of reduction and determined the ensuing attenuation of reperfusion-induced leukocyte adhesion. Furthermore, in WT mice treated with TNF-α, ~90% of rolling leukocytes progress to become adherent, and in E-selectin$^{-/-}$ mice where rolling velocities remain high, 50% of the rolling leukocytes are still able to adhere (44). There are several further explanations, which might account for these differences. In this study, we have looked at only CD11b expression and not CD11a, and it has been shown in Mac-1 (CD11b) KO mice that adhesion is normal due to the presence of CD11a (45); indeed, studies have shown that LFA-1 is the dominant of the two molecules with regard to neutrophil adhesion and migration (46). It is possible and likely that in vivo other adhesion molecules compensate for any reduction in ICAM-1 that might be present in Gal-$3^{-/-}$ mice. In support of this hypothesis, leukocyte trafficking is relatively normal in ICAM-1–deficient mice in a model of thioglycollate peritonitis (47), an effect that the authors proposed might be because of the ability of other adhesion molecules such as P- and E-selectin, LFA-1/ICAM-2, or α4β1 integrin. Interestingly, optimal rolling in vivo is reliant on ICAM-1, which might be the reason why differences are observed in KO mice with regard to rolling velocity rather than adhesion. Steeber et al. (48) have shown that at later time points during trauma-induced rolling in the cremaster (when P-selectin does not play such a dominant role), as well as in response to TNF-α stimulation, rolling velocities are significantly increased in ICAM-1 KO mice compared with WT. These studies and data presented in this article highlight the complex yet distinct nature of each step in the leukocyte recruitment cascade.

Our results in the parallel-plate flow chamber extend the findings of previous studies, which have focused on the end phase of transmigration. By using intravital microscopy and the parallel-plate flow chamber, we have been able to identify defects at earlier stages of the leukocyte recruitment cascade, namely rolling and activation. We have shown that Gal-$3^{-/-}$ leukocytes did not capture to E-selectin and initiate downstream changes in their activation state and cell morphology. To investigate this further, we examined the availability of E-selectin ligands in the absence of Gal-3 and determined that Gal-$3^{-/-}$ neutrophils displayed reduced HPA and PNA lectin binding, indicating that these cells have an altered cell surface glycophenotype. The importance of post-translational modification of E-selectin ligands to their functionality was recently demonstrated using mice lacking the polypeptide

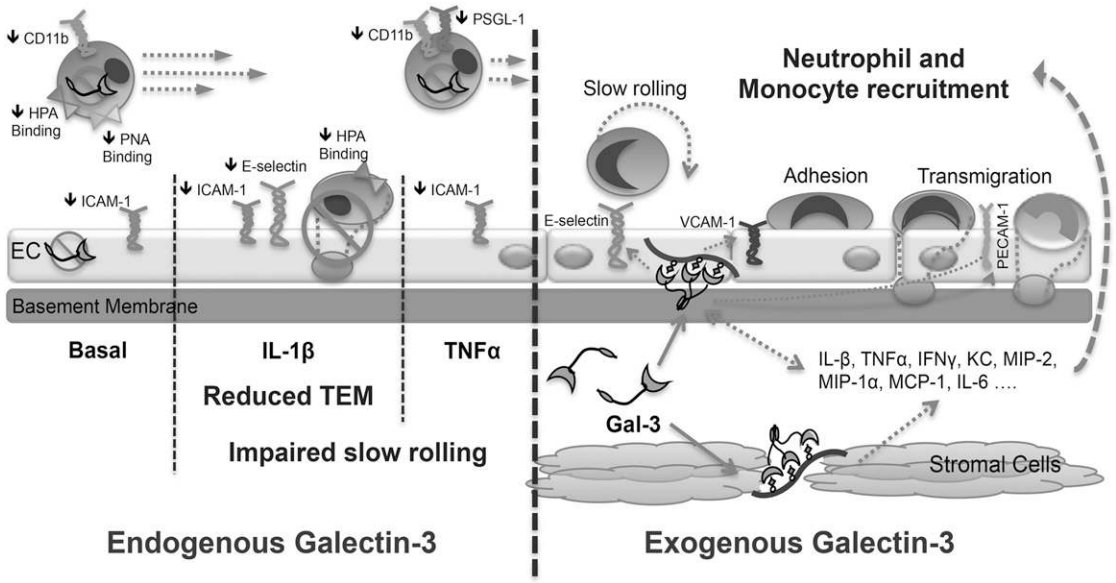

FIGURE 7. Gal-3 is a positive regulator of leukocyte recruitment to the inflamed microcirculation. In the absence of endogenous Gal-3 adhesion, molecule expression is reduced on circulating neutrophils and the vascular endothelium. The glycosylation profile of circulating neutrophils is also altered with reduced expression of glycans recognized by the lectins HPA and PNA. These changes correspond with impaired slow rolling of leukocytes in response to the cytokines TNF-α and IL-1β, with transendothelial migration in response to IL-1β also reduced. Conversely, administration of rGal-3 upregulates proinflammatory cytokines and chemokines, which results in the enhanced recruitment of neutrophils and monocytes into the tissue.

GalNAc transferase-1, which generates core-type *O*-glycan structures from GalNAc binding to threonine or serine residues in their protein backbone. Galnt-1$^{-/-}$ mice display reduced P- and E-selectin–mediated rolling, which in turn reduces adhesion and emigration of leukocytes in these animals; signaling through syk and thus integrin activation was unaffected, confirming that it is the ability of ligands to bind rather than downstream pathways that are impaired (49). Of particular importance in this study, Saravanan et al. (50) found that various glycogens were differentially expressed in Gal-3$^{-/-}$ mice undergoing a corneal model of wound healing; these included glycosyltransferases and glycosidases that were downregulated or upregulated to produce less *N*-glycans and more *O*-glycans. For example, an enzyme involved in Gal-3 ligand synthesis, β3-galactotransferase 5 (β3GalT5), was downregulated, whereas *N*-acetylgalactosaminyltransferases-3 and -7 (ppGalNAcTs-3 and -7), which initiate *O*-glycosylation, were upregulated (50).

It was important to observe that changes in lectin binding were specific with discreet alterations in HPA and PNA binding emerging from the assay analyses. HPA selectively binds to α-*N*-acetylgalactosamine residues and has been extensively studied as a marker of cancer cell metastasis (51). Another study highlighted the similar structure of HPA and sLe^x, hypothesizing they may have overlapping but not identical glycotopes (52), supporting the notion we propose in this article that reduced HPA binding indicates reduced selectin ligand binding. A putative receptor for PNA in keratinocytes is CD44, a known E-selectin ligand; this leads us to suggest that although CD44 levels are not reduced in Gal-3$^{-/-}$ leukocytes, they may display reduced binding capacity because of altered glycosylation (53).

Overall, our results suggest that there are defects in both the endothelial and the hematopoietic compartments in Gal-3$^{-/-}$ mice. This is evidenced by the reduced recruitment of Gal-3$^{-/-}$ leukocytes in the in vitro flow assay, as well as the greater defect in response to the endothelial-dependent stimulus IL-1β in vivo. One way to address this issue would be through the generation of bone marrow chimeras; however, we would anticipate from our results that defects in trafficking would be observed when Gal-3 is absent from either compartment, particularly if a global loss of Gal-3 results in an altered cellular glycophenotype. One way to address this issue would be to generate conditional KO mice, because this would enable the role of particular cellular sources of Gal-3 to be examined.

In the second part of this study, we have shown that exogenous Gal-3 elicits an inflammatory response alone, whereby local administration of rGal-3 to WT mice resulted in a dose-dependent reduction in rolling velocity associated with increased numbers of adherent and emigrated leukocytes, approximately half of which were Ly6G$^+$ neutrophils. i.s. administration of Gal-3 to CX$_3$CR1$^{gfp/+}$ mice confirmed that approximately equal numbers of monocytes are also recruited in response to this lectin. These findings are supported by numerous in vitro studies where Gal-3 acts as a chemoattractant for human neutrophils and monocytes in vitro and induces their recruitment to a mouse air-pouch model (54). Studies have also examined the role of Gal-3 in murine models of *S. pneumoniae* lung infection; accumulation of Gal-3 in the lungs correlated with neutrophil emigration to the alveoli during infection, and low levels of Gal-3 were bound to the neutrophil cell surface.

Our in vivo data have furthered our knowledge on the role of Gal-3 in leukocyte recruitment by extending its actions to monocyte recruitment as well as neutrophils. The effects of Gal-3 on monocyte migration have been further studied in vitro, where this lectin promoted monocyte chemotaxis, a finding replicated for human macrophages (55). Notably, Melo et al. (56) found that treatment of Gal-3 null sarcoma cells with rGal-3 increased migration on laminin, suggesting that any defects in the cells could be rescued. This rescue effect was not apparent in this study because treatment of Gal-3$^{-/-}$ leukocytes with physiological levels of rGal-3 in the ex vivo flow chamber assays were unable to reverse their phenotype and did not increase their capture to E-selectin under conditions of flow. Taken together with our findings that i.v. administration of Gal-3 did not affect leukocyte recruitment, this provides further evidence that, at least in these models and with the concentrations used in this study, a global lack of Gal-3 results in impaired leukocyte function in vivo.

Rather than acting directly on the leukocytes, the effect of exogenously delivered Gal-3 were indirect and lead to increased mRNA for IL-1β, TNF-α, KC, MCP-1, and IL-6 in the cremaster preparations. With the exception of IL-1β, these results were confirmed by proteome profile, which also revealed higher levels of IFN-γ, MIP-2, and MIP-1α post-Gal-3. These data point to stromal cells as the plausible target for Gal-3 to initiate a local inflammatory response. This is consistent with reports in the literature. Because levels of Gal-3 are increased at sites of joint destruction in rheumatoid arthritis, Filer et al. (57) investigated the effect of exogenous Gal-3 treatment of human synovial fibroblasts, which increased their production of IL-6, GM-CSF, TNF-α, and MMP-3, as well as the neutrophil chemoattractant IL-8 and the monocyte chemoattractants MCP-1, MIP-1α, and RANTES. The authors established that autocrine TNF-α stimulation was not the cause of this release; in fact, ERK MAPK activation occurred within 5 min, and JNK, p38 MAPK, and Akt phosphorylation were evident at 15 min, as well as activation of NF-κB. The activation of PI3K by Gal-3 has also been demonstrated in macrophages, which is often associated with chemokine production by stromal cells (58), as well as E-selectin–dependent neutrophil rolling and trafficking (59), both cell types that are abundant in the cremaster muscle.

Taken together, these results confirm that Gal-3 is a multifaceted molecule that exhibits modulatory properties on many aspects of the inflammatory response; based on our results, we propose the following model (Fig. 7) whereby the endogenous protein functions to potentiate the inflammatory response as evidenced by reduced adhesion molecule expression and an altered glycosylation profile culminating in a lack of slow rolling and reduced emigration in response to IL-1β. This is in contrast with exogenously administered Gal-3, which evokes a tissue-restricted circuit by acting on stromal cells (plausible ones are fibroblasts, macrophages, and endothelial cells), resulting in an enhanced proinflammatory state that culminates in increased levels of leukocyte trafficking. We propose that full definition of the roles for Gal-3 in controlling vascular inflammation can help in designing novel approaches for therapeutic benefit.

Acknowledgments

We would like to acknowledge the Consortium for Functional Glycomics from where breeding founders of the Gal-3$^{-/-}$ mouse colony were obtained.

Disclosures

The authors have no financial conflicts of interest.

References

1. Gilroy, D. W., T. Lawrence, M. Perretti, and A. G. Rossi. 2004. Inflammatory resolution: new opportunities for drug discovery. *Nat. Rev. Drug Discov.* 3: 401–416.
2. Serhan, C. N., S. D. Brain, C. D. Buckley, D. W. Gilroy, C. Haslett, L. A. O'Neill, M. Perretti, A. G. Rossi, and J. L. Wallace. 2007. Resolution of inflammation: state of the art, definitions and terms. *FASEB J.* 21: 325–332.
3. Hollingsworth, J. W., E. R. Siegel, and W. A. Creasey. 1967. Granulocyte survival in synovial exudate of patients with rheumatoid arthritis and other inflammatory joint diseases. *Yale J. Biol. Med.* 39: 289–296.
4. Ley, K., C. Laudanna, M. I. Cybulsky, and S. Nourshargh. 2007. Getting to the site of inflammation: the leukocyte adhesion cascade updated. *Nat. Rev. Immunol.* 7: 678–689.
5. Luster, A. D., R. Alon, and U. H. von Andrian. 2005. Immune cell migration in inflammation: present and future therapeutic targets. *Nat. Immunol.* 6: 1182–1190.
6. Barondes, S. H. V., V. Castronovo, D. N. Cooper, R. D. Cummings, K. Drickamer, T. Feizi, M. A. Gitt, J. Hirabayashi, C. Hughes, K. Kasai, et al. 1994. Galectins: a family of animal beta-galactoside-binding lectins. *Cell* 76: 597–598.
7. Cummings, R. D., I. S. Trowbridge, and S. Kornfeld. 1982. A mouse lymphoma cell line resistant to the leukoagglutinating lectin from *Phaseolus vulgaris* is deficient in UDP-GlcNAc: alpha-D-mannoside beta 1,6 N-acetylglucosaminyltransferase. *J. Biol. Chem.* 257: 13421–13427.
8. Ohshima, S., S. Kuchen, C. A. Seemayer, D. Kyburz, A. Hirt, S. Klinzing, B. A. Michel, R. E. Gay, F. T. Liu, S. Gay, and M. Neidhart. 2003. Galectin 3 and its binding protein in rheumatoid arthritis. *Arthritis Rheum.* 48: 2788–2795.
9. de Boer, R. A., D. J. Lok, T. Jaarsma, P. van der Meer, A. A. Voors, H. L. Hillege, and D. J. van Veldhuisen. 2011. Predictive value of plasma galectin-3 levels in heart failure with reduced and preserved ejection fraction. *Ann. Med.* 43: 60–68.
10. Lee, Y. J., S. W. Kang, J. K. Song, J. J. Park, Y. D. Bae, E. Y. Lee, E. B. Lee, and Y. W. Song. 2007. Serum galectin-3 and galectin-3 binding protein levels in Behçet's disease and their association with disease activity. *Clin. Exp. Rheumatol.* 25(4 Suppl. 45): S41–S45.
11. Sato, S., N. Ouellet, I. Pelletier, M. Simard, A. Rancourt, and M. G. Bergeron. 2002. Role of galectin-3 as an adhesion molecule for neutrophil extravasation during streptococcal pneumonia. *J. Immunol.* 168: 1813–1822.
12. Cooper, D., L. V. Norling, and M. Perretti. 2008. Novel insights into the inhibitory effects of Galectin-1 on neutrophil recruitment under flow. *J. Leukoc. Biol.* 83: 1459–1466.
13. Swamydas, M., and M. S. Lionakis. 2013. Isolation, purification and labeling of mouse bone marrow neutrophils for functional studies and adoptive transfer experiments. *J. Vis. Exp.* (77): e50586.
14. Reynolds, L. E., and K. M. Hodivala-Dilke. 2006. Primary mouse endothelial cell culture for assays of angiogenesis. *Methods Mol. Med.* 120: 503–509.
15. Pfaffl, M. W. 2001. A new mathematical model for relative quantification in real-time RT-PCR. *Nucleic Acids Res.* 29: e45.
16. Dinarello, C. A. 2011. A clinical perspective of IL-1β as the gatekeeper of inflammation. *Eur. J. Immunol.* 41: 1203–1217.
17. Dinarello, C. A. 2000. Proinflammatory cytokines. *Chest* 118: 503–508.
18. Schiff, M. H. 2000. Role of interleukin 1 and interleukin 1 receptor antagonist in the mediation of rheumatoid arthritis. *Ann. Rheum. Dis.* 59(Suppl. 1): i103–i108.
19. Kollias, G., E. Douni, G. Kassiotis, and D. Kontoyiannis. 1999. The function of tumour necrosis factor and receptors in models of multi-organ inflammation, rheumatoid arthritis, multiple sclerosis and inflammatory bowel disease. *Ann. Rheum. Dis.* 58(Suppl. 1): I32–I39.
20. Rampart, M., W. Fiers, W. de Smet, and A. G. Herman. 1989. Different pro-inflammatory profiles of interleukin 1 (IL 1) and tumor necrosis factor (TNF) in an in vivo model of inflammation. *Agents Actions* 26: 186–188.
21. Kunkel, E. J., and K. Ley. 1996. Distinct phenotype of E-selectin-deficient mice. E-selectin is required for slow leukocyte rolling in vivo. *Circ. Res.* 79: 1196–1204.
22. Simon, S. I., Y. Hu, D. Vestweber, and C. W. Smith. 2000. Neutrophil tethering on E-selectin activates beta 2 integrin binding to ICAM-1 through a mitogen-activated protein kinase signal transduction pathway. *J. Immunol.* 164: 4348–4358.
23. Functional Glycomics Gateway. Mouse line phenotype analysis. Available at: http://www.functionalglycomics.org/glycomics/publicdata/phenotyping.jsp. Accessed: February 25, 2016.
24. Young, R. E., R. D. Thompson, and S. Nourshargh. 2002. Divergent mechanisms of action of the inflammatory cytokines interleukin 1-beta and tumour necrosis factor-alpha in mouse cremasteric venules. *Br. J. Pharmacol.* 137: 1237–1246.
25. Kuwabara, I., and F. T. Liu. 1996. Galectin-3 promotes adhesion of human neutrophils to laminin. *J. Immunol.* 156: 3939–3944.
26. Nieminen, J., A. Kuno, J. Hirabayashi, and S. Sato. 2007. Visualization of galectin-3 oligomerization on the surface of neutrophils and endothelial cells using fluorescence resonance energy transfer. *J. Biol. Chem.* 282: 1374–1383.
27. Yang, R. Y., D. K. Hsu, and F. T. Liu. 1996. Expression of galectin-3 modulates T-cell growth and apoptosis. *Proc. Natl. Acad. Sci. USA* 93: 6737–6742.
28. Fukumori, T., Y. Takenaka, T. Yoshii, H. R. Kim, V. Hogan, H. Inohara, S. Kagawa, and A. Raz. 2003. CD29 and CD7 mediate galectin-3-induced type II T-cell apoptosis. *Cancer Res.* 63: 8302–8311.
29. Bhaumik, P., G. St-Pierre, V. Milot, C. St-Pierre, and S. Sato. 2013. Galectin-3 facilitates neutrophil recruitment as an innate immune response to a parasitic protozoa cutaneous infection. *J. Immunol.* 190: 630–640.
30. Nieminen, J., C. St-Pierre, P. Bhaumik, F. Poirier, and S. Sato. 2008. Role of galectin-3 in leukocyte recruitment in a murine model of lung infection by *Streptococcus pneumoniae*. *J. Immunol.* 180: 2466–2473.
31. Jiang, H. R., Z. Al Rasebi, E. Mensah-Brown, A. Shahin, D. Xu, C. S. Goodyear, S. Y. Fukada, F. T. Liu, F. Y. Liew, and M. L. Lukic. 2009. Galectin-3 deficiency reduces the severity of experimental autoimmune encephalomyelitis. *J. Immunol.* 182: 1167–1173.
32. Hsu, D. K., R. Y. Yang, Z. Pan, L. Yu, D. R. Salomon, W. P. Fung-Leung, and F. T. Liu. 2000. Targeted disruption of the galectin-3 gene results in attenuated peritoneal inflammatory responses. *Am. J. Pathol.* 156: 1073–1083.
33. Colnot, C., M. A. Ripoche, G. Milon, X. Montagutelli, P. R. Crocker, and F. Poirier. 1998. Maintenance of granulocyte numbers during acute peritonitis is defective in galectin-3-null mutant mice. *Immunology* 94: 290–296.
34. Farnworth, S. L., N. C. Henderson, A. C. Mackinnon, K. M. Atkinson, T. Wilkinson, K. Dhaliwal, K. Hayashi, A. J. Simpson, A. G. Rossi, C. Haslett, and T. Sethi. 2008. Galectin-3 reduces the severity of pneumococcal pneumonia by augmenting neutrophil function. *Am. J. Pathol.* 172: 395–405.
35. Ge, X. N., N. S. Bahaie, B. N. Kang, M. R. Hosseinkhani, S. G. Ha, E. M. Frenzel, F. T. Liu, S. P. Rao, and P. Sriramarao. 2010. Allergen-induced airway remodeling is impaired in galectin-3-deficient mice. *J. Immunol.* 185: 1205–1214.
36. Ge, X. N., S. G. Ha, F. T. Liu, S. P. Rao, and P. Sriramarao. 2013. Eosinophil-expressed galectin-3 regulates cell trafficking and migration. *Front. Pharmacol.* 4: 37.
37. Woodfin, A., M. B. Voisin, B. A. Imhof, E. Dejana, B. Engelhardt, and S. Nourshargh. 2009. Endothelial cell activation leads to neutrophil transmigration as supported by the sequential roles of ICAM-2, JAM-A, and PECAM-1. *Blood* 113: 6246–6257.

38. Koenen, R. R., J. Pruessmeyer, O. Soehnlein, L. Fraemohs, A. Zernecke, N. Schwarz, K. Reiss, A. Sarabi, L. Lindbom, T. M. Hackeng, et al. 2009. Regulated release and functional modulation of junctional adhesion molecule A by disintegrin metalloproteinases. *Blood* 113: 4799–4809.
39. Feduska, J. M., P. L. Garcia, S. B. Brennan, S. Bu, L. N. Council, and K. J. Yoon. 2013. N-glycosylation of ICAM-2 is required for ICAM-2-mediated complete suppression of metastatic potential of SK-N-AS neuroblastoma cells. *BMC Cancer* 13: 261.
40. Newton, J. P., A. P. Hunter, D. L. Simmons, C. D. Buckley, and D. J. Harvey. 1999. CD31 (PECAM-1) exists as a dimer and is heavily N-glycosylated. *Biochem. Biophys. Res. Commun.* 261: 283–291.
41. Dangerfield, J. P., S. Wang, and S. Nourshargh. 2005. Blockade of alpha6 integrin inhibits IL-1beta- but not TNF-alpha-induced neutrophil transmigration in vivo. *J. Leukoc. Biol.* 77: 159–165.
42. Norman, K. E., A. G. Katopodis, G. Thoma, F. Kolbinger, A. E. Hicks, M. J. Cotter, A. G. Pockley, and P. G. Hellewell. 2000. P-selectin glycoprotein ligand-1 supports rolling on E- and P-selectin in vivo. *Blood* 96: 3585–3591.
43. Kubes, P., M. Jutila, and D. Payne. 1995. Therapeutic potential of inhibiting leukocyte rolling in ischemia/reperfusion. *J. Clin. Invest.* 95: 2510–2519.
44. Kunkel, E. J., J. L. Dunne, and K. Ley. 2000. Leukocyte arrest during cytokine-dependent inflammation in vivo. *J. Immunol.* 164: 3301–3308.
45. Lu, H., C. W. Smith, J. Perrard, D. Bullard, L. Tang, S. B. Shappell, M. L. Entman, A. L. Beaudet, and C. M. Ballantyne. 1997. LFA-1 is sufficient in mediating neutrophil emigration in Mac-1-deficient mice. *J. Clin. Invest.* 99: 1340–1350.
46. Ding, Z. M., J. E. Babensee, S. I. Simon, H. Lu, J. L. Perrard, D. C. Bullard, X. Y. Dai, S. K. Bromley, M. L. Dustin, M. L. Entman, et al. 1999. Relative contribution of LFA-1 and Mac-1 to neutrophil adhesion and migration. *J. Immunol.* 163: 5029–5038.
47. Steeber, D. A., M. L. Tang, N. E. Green, X. Q. Zhang, J. E. Sloane, and T. F. Tedder. 1999. Leukocyte entry into sites of inflammation requires overlapping interactions between the L-selectin and ICAM-1 pathways. *J. Immunol.* 163: 2176–2186.
48. Steeber, D. A., M. A. Campbell, A. Basit, K. Ley, and T. F. Tedder. 1998. Optimal selectin-mediated rolling of leukocytes during inflammation in vivo requires intercellular adhesion molecule-1 expression. *Proc. Natl. Acad. Sci. USA* 95: 7562–7567.
49. Block, H., K. Ley, and A. Zarbock. 2012. Severe impairment of leukocyte recruitment in ppGalNAcT-1-deficient mice. *J. Immunol.* 188: 5674–5681.
50. Saravanan, C., Z. Cao, S. R. Head, and N. Panjwani. 2009. Detection of differentially expressed wound-healing-related glycogenes in galectin-3-deficient mice. *Invest. Ophthalmol. Vis. Sci.* 50: 5690–5696.
51. Rambaruth, N. D., P. Greenwell, and M. V. Dwek. 2012. The lectin Helix pomatia agglutinin recognizes O-GlcNAc containing glycoproteins in human breast cancer. *Glycobiology* 22: 839–848.
52. Köhler, S., S. Ullrich, U. Richter, and U. Schumacher. 2010. E-/P-selectins and colon carcinoma metastasis: first in vivo evidence for their crucial role in a clinically relevant model of spontaneous metastasis formation in the lung. *Br. J. Cancer* 102: 602–609.
53. Hudson, D. L., J. Sleeman, and F. M. Watt. 1995. CD44 is the major peanut lectin-binding glycoprotein of human epidermal keratinocytes and plays a role in intercellular adhesion. *J. Cell Sci.* 108: 1959–1970.
54. Sano, H., D. K. Hsu, L. Yu, J. R. Apgar, I. Kuwabara, T. Yamanaka, M. Hirashima, and F. T. Liu. 2000. Human galectin-3 is a novel chemoattractant for monocytes and macrophages. *J. Immunol.* 165: 2156–2164.
55. Danella Polli, C., K. Alves Toledo, L. H. Franco, V. Sammartino Mariano, L. L. de Oliveira, E. Soares Bernardes, M. C. Roque-Barreira, and G. Pereira-da-Silva. 2013. Monocyte migration driven by galectin-3 occurs through distinct mechanisms involving selective interactions with the extracellular matrix. *ISRN Inflamm.* 2013: 259256.
56. Melo, F. H., D. Butera, Mde. S. Junqueira, D. K. Hsu, A. M. da Silva, F. T. Liu, M. F. Santos, and R. Chammas. 2011. The promigratory activity of the matricellular protein galectin-3 depends on the activation of PI-3 kinase. *PLoS One* 6: e29313.
57. Filer, A., M. Bik, G. N. Parsonage, J. Fitton, E. Trebilcock, K. Howlett, M. Cook, K. Raza, D. L. Simmons, A. M. Thomas, et al. 2009. Galectin 3 induces a distinctive pattern of cytokine and chemokine production in rheumatoid synovial fibroblasts via selective signaling pathways. *Arthritis Rheum.* 60: 1604–1614.
58. MacKinnon, A. C., S. L. Farnworth, P. S. Hodkinson, N. C. Henderson, K. M. Atkinson, H. Leffler, U. J. Nilsson, C. Haslett, S. J. Forbes, and T. Sethi. 2008. Regulation of alternative macrophage activation by galectin-3. *J. Immunol.* 180: 2650–2658.
59. Puri, K. D., T. A. Doggett, C. Y. Huang, J. Douangpanya, J. S. Hayflick, M. Turner, J. Penninger, and T. G. Diacovo. 2005. The role of endothelial PI3Kgamma activity in neutrophil trafficking. *Blood* 106: 150–157.